

## Chitosan-Curcumin Coating Characterization on Cobalt-Chrome Surface by 100 kHz Ultrasonic Spray Method

K. I. Muttaqin\*

Department of Mechanical and Industrial Engineering, Faculty of Engineering, Universitas Gadjah Mada. Jl. Grafika 2, Yogyakarta 55281, Indonesia

Email:

\*katiko.imamul.m@mail.ugm.ac.id

### Keywords

curcumin, stent, coating, ultrasonic spray.

### Abstract

Curcumin possesses anticoagulant, anti-proliferative, and anti-inflammatory properties and is applicable to prevent in-stent restenosis. This research investigated curcumin coating with biodegradable chitosan polymer as a drug carrier universally made on Co-Cr L605 surface by the ultrasonic spray method. Three curcumin doses were implemented: low dose (150  $\mu\text{g}$  of curcumin per sample), medium dose (300  $\mu\text{g}$  of curcumin per sample), and high dose (480  $\mu\text{g}$  of curcumin per sample). The metal surface morphologies before and after coating were examined by using a stylus profilometer and a scanning electron microscope (SEM). The result showed that coating films were formed fine and uniform with an average roughness level below 0.2  $\mu\text{m}$ . The coating film structure characterization by Fourier-transform infrared (FTIR) spectroscopy showed that curcumin absorption spectra still occurred in the chitosan-curcumin coating, although chitosan strong absorption spectra were dominant.

## 1. Introduction

Atherosclerosis is a primary cause of the coronary heart disease, with fat and cholesterol build-up which can lead to narrowing of coronary blood vessels and eventually blocking the blood circulation. Such a fat and cholesterol accumulations also cause blood clotting that can trigger myocardial infarction (Mendis et al., 2011). Several treatments have been implemented to tackle coronary heart disease, such as angioplasty, coronary bypass surgery, and stent placement. The last of the three aforementioned treatments is the most popular option due to its advantages in terms of ease, speed, and post-installation effect. Furthermore, this treatment is also highly effective in preventing restenosis, which usually occurs in the bypass treatment (Erbel et al., 1998).

Bare-metal stent (BMS) is a first-generation stent which has been implemented into a blocked coronary blood vessel. It is a hollow tube made of stainless steel (SS) 316L, cobalt-chromium (Co-Cr), magnesium, and tantalum (Schiavone et al., 2014), that is designed for opening up blood clots by installing it into the vessel with the aid of an angioplasty balloon (Tan et al., 2016). Although it is able to overcome blood clotting, it brings about a new issue called in-stent restenosis (ISR) with the passing time. ISR occurs with the growth of smooth muscle cells on the inner wall of the vessel as the body's protective action against incoming foreign objects. Such a cell growth leads to a new problem with the blood vessel lumen growing narrower and eventually closed up again (Curcio et al., 2011).

The importance of the ISR urges an alternative way to curb or slow down the smooth muscle cell growth. One of the techniques that has so far been used is by coating the BMS with an anti-restenosis drug; which is often called drug-eluting stent (DES). This technique can be achieved by coating with a polymer mix as a carrier and serves in the drug binding. Spray coating can be used to achieve this purpose in addition to other

methods such as dip coating, electrophoretic deposition (EPD), and layer-by-layer coating (Livingston et al., 2016).

DES is first applied by using a biostable polymer, which is a mix of polyethylene-co-vinyl acetate (PEVA), poly-n-butyl methacrylate (PBMA) as a carrier, and sirolimus as an anti-proliferative drug. It was reported that DES have successfully decreased restenosis rates better than BMS over a 6-month period (Martin and Boyle, 2011) owing to a better treatment ability than BMS (Tontowi et al., 2013).

The non-degradable polymer in DES would however result in thrombosis within a certain time span (Khan et al., 2012). Hence, the use of such bioabsorbable polymers have been introduced to replace non-degradable DES, such as those from PLGA, PLLA, and PET, which are degradable after a time period, or chitosan, which is a naturally bioabsorbable polymer and largely produced from crab shell waste.

Mohan et al. (2016) conducted a study on chitosan as a DES carrier with quercetin serving as a coating drug on TiO<sub>2</sub> nanotubes. The increase in the chitosan concentration applied would slow down the drug release. Another investigation on chitosan as a carrier with paclitaxel serving as drug was conducted by Tang et al. (2017). The results showed that the functional groups of the paclitaxel chemical bond were still present in the chitosan-paclitaxel mix. This was as evidenced by the existence of paclitaxel absorption spectra within the paclitaxel-chitosan co-assembly.

As reported by Nurdjaman (2003), four species of *Curcuma* can be encountered in Indonesia: *Curcuma aeruginosa* Roxb (black turmeric), *Curcuma domestica* Val (turmeric), *Curcuma heyreana* (pale turmeric), and *Curcuma xanthorrhiza* Roxb (Javanese turmeric). *Curcuma* is composed of some bioactive compounds, curcumin being the most prominent, and it has the molecular formula C<sub>21</sub>H<sub>20</sub>O<sub>6</sub>. Pan et al. (2006) performed an investigation into coating on SS 316LVM stent with PLGA as drug carrier and

curcumin as drug with varied drug dosages at 10%, 20%, and 35%. The study found that the curcumin-PLGA co-assembly featured spectra which indicated the functional groups found in curcumin and those in PLGA. This proved that in the curcumin-PLGA mixture there is no new chemical reactions occurring and no curcumin vanishes from this mixture. Curcumin per se comes with anticancer, anti-inflammatory, antibacterial, and anti-arteriosclerosis abilities and is safe to consume in a high amount (Fryer et al., 2009). In this research, therefore, curcumin was used as the drug, while chitosan as the drug carrier.

## 2. Materials and Methods

### 2.1. Materials

In this research, Gamayasa Inastent made of Co-Cr L605 tube was used. Curcumin was purchased from Merck. Inc. with  $\geq 75.0\%$  purity (HPLC grade). Chitosan ( $\geq 75\%$  DDA and 310,000–375,000 Da MW) was obtained from Sigma-Aldrich Inc. All other reagents used in this research were of analytical grade.

### 2.2. Nanotube Preparation

To prepare Co-Cr nanotube, a Co-Cr L605 tube were first put into an ingot until its melting point was reached. The Co-Cr L605 melt was then poured into a sample nanotube cast 6 in diameter and 2 mm in height. After the Co-Cr L605 melt solidified, it was then quenched with water. Annealing was then conducted at 1000 °C for 1 hour, and cooling was conducted in an electrical furnace. The sample was polished using a piece of 800–5000 mesh SiC paper. The annealed nanotube was cleaned in an ultrasonic bath using acetone, ethanol, and water in turn (Herliansyah et al., 2017). The cleaned nanotube was dried in an oven for a 6-hour drying process.

### 2.3. Curcumin-chitosan coating preparation

Curcumin-chitosan solutions were prepared by homogenizing 0.25% w/v chitosan in three curcumin doses, i.e., low, medium, and high. The amounts of curcumin and chitosan used are shown in Table 1. The

curcumin-chitosan solutions were kept in solution containers and then converted into aerosol form by 100 kHz ultrasonic atomizer and sprayed to the Co-Cr surface. It is worth noting that not all solutions would cling to the stent surface during the spraying process.

### 2.4. Functional groups of the curcumin film

The curcumin-chitosan solutions that were prepared was sprayed on the Co-Cr nanotube surface and dried in the oven at 40 °C for 1 hour. Then the dry films formed were removed from the nanotube surface for examination by Perkin Elmer Paragon 1000 PC FTIR (Fourier-transform infrared) spectrometer across the scanning span 4000  $\text{cm}^{-1}$  to 400  $\text{cm}^{-1}$ .

### 2.5. Sample surface morphology

The curcumin-chitosan coating surface morphology of the stent surface was examined by SEM (scanning electron microscopy), Carl Zeiss, Evo MA 10.

### 2.6. Coating surface roughness

Surface roughness was to be examined using a stylus profilometer, SE300. This was conducted by examining the Co-Cr nanotube sample surface before and after the spraying process to find out the roughness of the curcumin-chitosan coating formed.

Table 1. Curcumin and chitosan amounts used in this research

Dose	90% Curcumin ( $\mu\text{g}/\text{ml}$ )	10% Chitosan ( $\mu\text{g}/\text{ml}$ )
Low	150	250
Medium	500	250
High	800	250

## 3. Results and Discussion

The chitosan coating with curcumin on the Co-Cr metal surface was observed using SEM. Figure 2 illustrates the SEM process of the stent coating. The stent surface that was coated with curcumin had a cracked film and many particles all around it. Using Image-J analysis, the curcumin particle was

measured of having sizes between 0.5 – 1  $\mu\text{m}$ . Meanwhile, the stent surface that was coated with chitosan exhibited undulation on it. There was no crack on the surface, and the chitosan particles were distributed uniformly

throughout the stent surface. On the stent surface that was coated with the curcumin-chitosan mix, curcumin particles were found to cling to chitosan particles and be uniformly distributed.

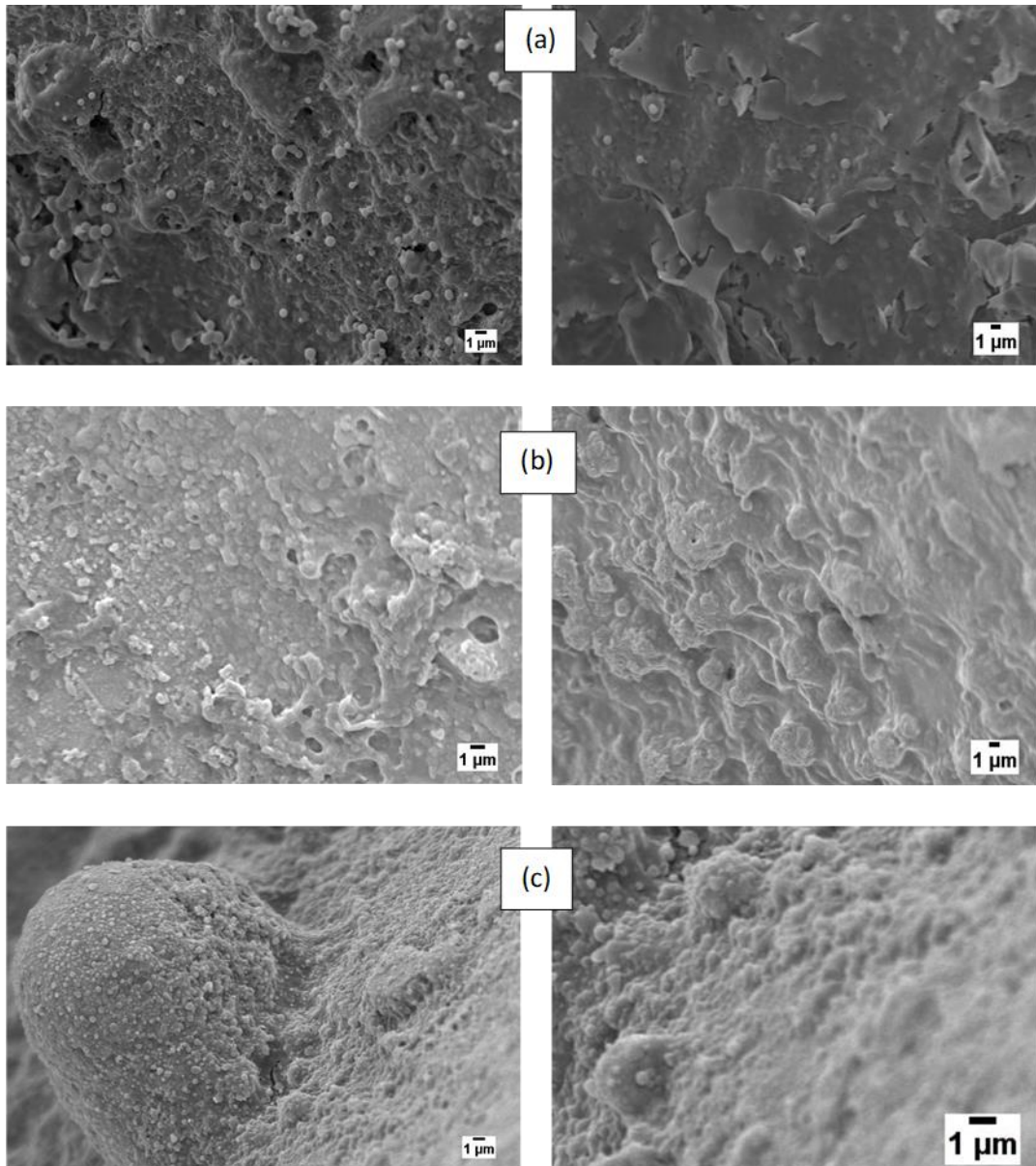


Figure 1. SEM coating on Co-Cr surface (a) curcumin coating; (b) chitosan coating; (c) curcumin-chitosan coating

The presence of curcumin on the coating film that formed was confirmed by FTIR spectroscopy as presented in Figure 2.

The result of the chitosan FTIR spectroscopy showed three dominant absorptions: at 3500  $\text{cm}^{-1}$ , showing the presence of the O–H

hydroxyl group; at  $1100\text{ cm}^{-1}$ , showing the presence of the C–O–C group; and at  $1620\text{ cm}^{-1}$ , showing the presence of the  $\text{–NH}_2$  amide group (Shahbazi et al., 2013). As for the curcumin FTIR spectroscopy, the result showed that there were absorptions at  $3500\text{ cm}^{-1}$ , showing the O–H alcohol group, and at  $1600\text{ cm}^{-1}$ , showing the C=C aromatic double bond (Pan et al., 2006). There was also an absorption at around  $2800\text{ cm}^{-1}$  to  $3000\text{ cm}^{-1}$ , which was indicative of the presence of the  $\text{–C–H}$  ( $\text{Csp}^3$ ) hydrocarbon group. Furthermore, an absorption occurred at around  $1370\text{ cm}^{-1}$  to  $1450\text{ cm}^{-1}$ , indicating the  $\text{–CH}_3$  methyl group, and a strong absorption occurred at around  $1000\text{ cm}^{-1}$ , indicating the  $\text{–C–O}$  group.

Meanwhile, based on the curcumin-chitosan FTIR spectra, the absorptions were dominated by the chitosan spectra with three dominant absorptions: at around  $3500\text{ cm}^{-1}$ , showing the presence of the O–H hydroxyl group; at around  $1100\text{ cm}^{-1}$ , showing the presence of the C–O–C group; and at around  $1620\text{ cm}^{-1}$ , showing the presence of the  $\text{–NH}_2$  group. However, some functional groups in curcumin like the  $\text{–OH}$  alcohol group, the C=C group, the  $\text{–C–H}$  group, the  $\text{–CH}_3$  group, and the  $\text{–C–O}$  group were also present in the curcumin-chitosan FTIR spectra. The mixing of the two did not raise a new chemical reaction as proven by the absence of a new absorption in the mix.

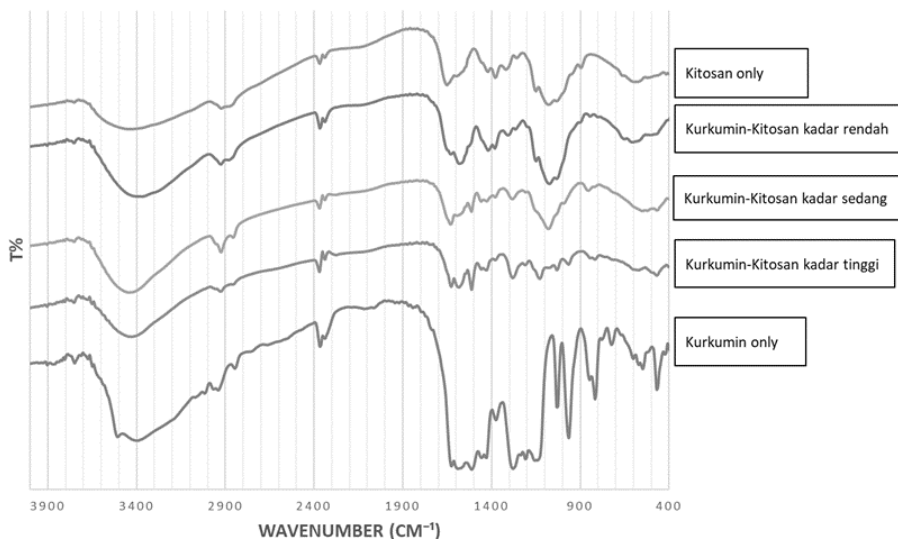


Figure 2. Curcumi-chitosan coating FTIR spectra

The variation in the curcumin doses used in the coating yielded varied levels of surface roughness. Prior to the spraying, the surface roughness ( $R_a$ ) of all the samples were measured at  $0.02\text{ }\mu\text{m}$ . After the spraying, some increases were observed in the surface

roughness. Figure 3 shows the samples' surface roughness before and after spraying. The surface roughness ( $R_a$ ) after spraying was  $0.07\text{ }\mu\text{m}$  for the low dose,  $0.11\text{ }\mu\text{m}$  for the medium dose, and  $0.13\text{ }\mu\text{m}$  for the high dose.

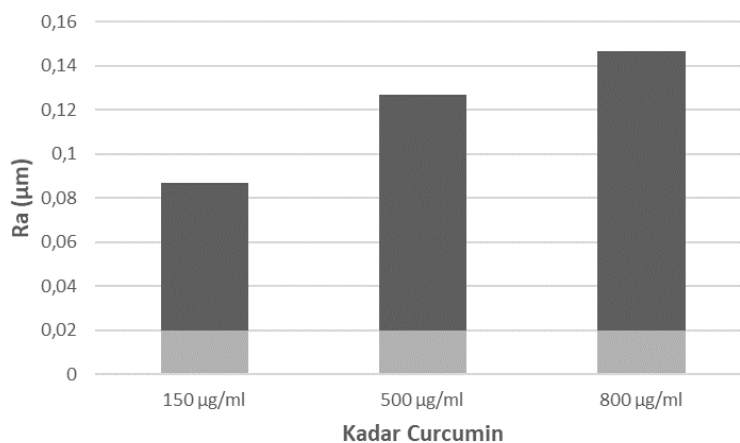


Figure 3. Co-Cr surface roughness before and after curcumin-chitosan coating

The increases were in direct proportion with the increases in the curcumin doses used. In support of this finding, the SEM result showed greater quantities of small particles (curcumin) spread all over the samples' surface with the increases in the curcumin doses used. These curcumin small particles were also influenced by the solidification that occurred shortly after the spraying (Peng and Liu, 2001).

#### 4. Conclusion

The co-assembly of curcumin and chitosan did not lead to a new chemical reaction as marked by the presence of the –OH alcohol group, the C=C group, the –C–H group, the –CH<sub>3</sub> group, and the –C–O group that compose curcumin, although chitosan strong spectra still dominated. Curcumin-chitosan coating on Co-Cr L605 surface at varied curcumin doses yielded varying levels of roughness. The increases in the samples' surface roughness were directly proportionate to the increase in the curcumin doses used for the coating.

#### 5. References

- Curcio A., Torella D., & Indolfi C., 2011, Mechanisms of smooth muscle cell proliferation and endothelial regeneration after vascular injury and stenting, *Circulation Journal*, Vol. 75, pp. 1287 – 1296
- Fryer, R., Galustian, C., & Dalgelish, A., 2009, Recent advances and developments in treatment strategies against pancreatic cancer, *Current Clinical Pharmacology*, Vol. 4, pp. 102–112.
- Erbel, R., Haude, M., Hopp, H. W., Franzen, D., Rupprecht, H. J., & Heublein, P. P., 2011, Coronary-artery stenting compared with balloon angioplasty for restenosis after initial balloon angioplasty, *Survey of Anesthesiology*, Vol. 43, pp. 195–196.
- Herliansyah, M. K., Ilman, K. A., & Tontowi, A. E., 2017, Potential of curcumin as antiproliferative drug for developing drug eluting stent : a brief review, international conference on instrumentation, Communications, Information Technology and Biomedical Engineering, Vol. 978, pp. 5386-3455.
- Khan. W., Farah. S., & Domb. A.J., 2012, Drug eluting stents : developments and current status, *Journal of Controlled Release*, Vol. 161, pp. 703 – 712.
- Livingston, M., & Tan, A., 2016, Coating techniques and release kinetics of drug-eluting stents, *Journal of Medical Devices*, vol. 10, pp. 010801-1 - 010801-8.

- Martin, D. M., & Boyle, F. J., 2011, Drug-eluting stents for coronary artery disease: a review, *Medical Engineering & Physics*, Vol. 33, pp. 148–163.
- Mendis S., Puska P., & Norrving Bo., 2011, *Global atlas on cardiovascular disease prevention and control*, World Health Organization.
- Nurdjaman, I. H., 2003, *Manfaat curcumin pada nyeri punggung bawah akut miofasial*, Master Thesis, Universitas Gadjah Mada.
- Pan, Ch. J., Tang, J. J., Weng, Y. J., Wang, J., & Huang, N., 2006, Preparation, characterization and anticoagulation of curcumin-eluting controlled biodegradable coating stents, *Journal of Controlled Release*, Vol. 116, pp. 42–49.
- Peng, Z., & Liu, M., 2001, preparation of dense platinum-yttria stabilized zirconia and yttria stabilized zirconia films on porous  $\text{La}_{0.9}\text{Sr}_{0.1}\text{MnO}_3$  (LSM) substrates, *Journal of the American Ceramic Society*, Vol. 84, pp. 283–88.
- Shahbazi, M. A., Hamidi, M., & Mohammadi-Samani, S. (2013). Preparation, optimization, and in-vitro/in-vivo/ex-vivo characterization of chitosan-heparin nanoparticles: drug-induced gelation. *Journal of Pharmacy and Pharmacology*, Vol. 65, pp. 1118-1133.
- Tan C., & Schatz R.A., 2016, The history of coronary stenting, *Intervention Cardiology Clinic*, vol. 5, pp. 271 – 280.
- Tontowi, A. E., Ikra, P., & Siswomihardjo, W. 2013. Mapping of coronary stent demand of several hospitals in Indonesia and its forecasting, *Proc. of 2013 3rd Int. Conf. on Instrumentation, Communications, Information Technol., and Biomedical Engineering: Science and Technol. for Improvement of Health, Safety, and Environ., ICICI-BME*, pp. 436–439.